# Performance improvement of IF(CN2)2 meta based N-channel OTFTs and their integration into a stable CMOS inverter

S. Bebiche, I. Bouhadda, T. Mohammed-Brahim, N. Coulon, Jean-Francois Bergamini, Cyril Poriel, Emmanuel Jacques

# Performance improvement of $IF(CN_2)_2$ meta based N-channel OTFTs and their integration into a stable CMOS inverter

S.Bebiche[1,2], I.Bouhadda[1], T.Mohammed-Brahim[1], N.Coulon[1], J.F.Bergamini[3], C.Poriel[3], E.Jacques[1]

[1]*UMR CNRS 6164-Institut d'Électronique et des Télécommunications de Rennes-Département Microélectronique &Microcapteurs, Bât.11B, Université Rennes 1, Campus de Beaulieu 35042 Rennes Cedex, France*

[2] *State Key Laboratory, ECE department, Hong Kong University of Science and Technology, Clear Water Bay, Hong Kong.*

[3] *UMR CNRS 6226-Institut des Sciences Chimiques de Rennes- Équipe Matière Condensée et Systèmes Électroactifs, Bat 10C, Campus de Beaulieu - 35042 Rennes cedex France*

**Abstract**

In this work we report on the fabrication of N channel transistors based on $IF(CN_2)_2$ meta molecule.The effect of $IF(CN_2)_2$ meta evaporation parameters on corresponding TFTs performances, is evaluated and highlighted here. Since the effect of deposition conditions for this molecule type has not been reported yet, here we report an improvement about 20 times of field effect mobility when deposited at substrate temperature of 80 °C and deposition rate of 0.7A °/s, then annealed at low temperature. Reached mobility of $2.2x10^{-3}cm^2/V.s$,is comparable to reported $\mu_{FE}$of single crystal indenofluorene TFTs.The optimum mobility in these evaporation conditions was explained by the best compromise between the grain size and packing density of films. Fabricated $IF(CN_2)_2$ meta based devices are combined to 6,13-Bis(triisopropylsilylethynyl)pentacene devices and then integrated into a CMOS inverter logic circuit.Theinverter'sVTC shows large output voltage swing. Electrical stability of the performed inverter was also evaluated and the inverter shows a correct electrical stability,

after 3 hours of non-stop operation the peak to peak magnitude corresponding to $V_{OUT}$ decreases only by 2.6%.

## 1. Introduction

Organic electronic has attracted some interest due to thepotential advantages that it offers such as low temperature processing, flexibility, printability,affordable production cost and the ease to perform devices compared to classical electronics [1-5]. During the last decadesmany applications were successfully achieved using the fundamental circuit element; organic TFT, these applications includegas sensing [6,7], AMOLED display addressing [8] and logic gate circuits such as CMOS[9, 10] or CMOS-like inverters[11]. For low power consumption systems, logic Complementary MOS circuits are preferred.These require the use of both P and N channel transistors. A great deal of progress was made with P channel transistors.Indeed mobility from 1-5 $cm^2/V.s$ has already been reported for evaporated molecules [12]. Until now performing N channeltransistors with interesting mobility and stability has been a real challenge. Because of poor electronic transport in their active layers, N channel transistors commonly present low field effect mobility and electrical stability. This constitutes a serious obstacle to achieving CMOS circuits.

Regarding the mobility, a closer look at the molecule design highlighted the effect of molecule's geometry on its electrical properties. In fact a variety of studies on N channel materials reported the effect of the molecule geometry on its electrical properties [13,14]. It has been demonstrated that planar geometry of molecules, such as Thiophene-Naphtalene molecules [14], promotes the π-π stacking of molecular orbitals. On the other hand a strong π stacking leads an improvement in the electronic hopping over the system,thus the mobility can be increased [15]. Another approach to enhance the field effect mobility consists of

improving the elaboration conditions of the active layer. In case of evaporated molecules, it is obvious that deposition parameters such as temperature deposition or deposition rates have an impact on the film growth [14,16-20], which is directly correlated to the electronic transport. In fact, large grain structure and packing grain density lead to a high field effect mobility.

In this work themolecule used for the active layer is an indenofluorene derivative ($IF(CN_2)_2$-meta). This molecule is characterized by a planar geometry and deep LUMO energy level.Some studies on indenofluorene derivatives reported N channel transistors with a saturated mobility of $3x10^{-3}cm^2/V.s$ for crystal OFETs [21], while 0.16 $cm^2/V.s$ are reached for an active layer deposited using the epitaxial method [22]. However no application of these transistors as an element of CMOS logic gate circuit was demonstrated.

Herein we report on the integration of evaporated $IF(CN_2)_2$-meta-based OTFTs devices, in CMOS inverter circuits and their electrical stability.Several papers focused onN channel transistors with high mobility, in which organic circuits were performed.However these transistors are lacking electrical stability when integrated into circuits. In this paper we start by an optimization study on the N channel transistor which deals with the effects of deposition parameters of $IF(CN_2)_2$-meta molecule and post annealing treatment, on OTFT's field effect mobility. Once N channel devices are optimized, they are combined to Tips-Pentacene-based devices, and used to perform an organic CMOS inverter, possessing good time stability under voltage polarization.

## 2. Materials and methods

Bottom gate bottom contact transistors are performed on previously cleaned glass substrate, with acetone and ethanol-alcohol rinsing. To define the gate contact, 150nm evaporated aluminum layer is followed by a photolithography step. SU-8 photoresist is spin coated at 320nm and used as agate dielectric in order to avoid leakage current and to make a smooth

interface with the active layer. Source and drain contacts are defined using photolithography on 60nm evaporated gold.Finally SU-8 is etched on vias zones. The last step consists of thermal evaporation of 8nm of IF $(CN_2)_2$ meta molecule, under high vacuum with controlled conditions ($p=3.10^{-7}$mbar ,$T_{sub}$=30°C and $d_r$=0.4A°/s).

As announced above, IF$(CN_2)_2$ meta molecule (Figure 1) is characterized by a planar geometry and deep LUMO energy level, measured at -3.81eV. This deep LUMO level resulted from the introduction of $(CN_2)$ electro-attractive groups. Notethat this molecule's band gap is 2.1eVand large enough to avoid minority carrier injections from the source/drain metal which may contribute to an increase the OFF drain source current. More information about IF$(CN_2)_2$ meta synthesis and chemical characterization can be found in a previous paper [23].

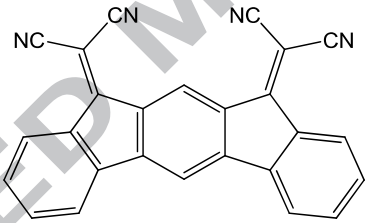


Figure 1: Chemical structure of IF $(CN_2)_2$ meta molecule

## 3. Results and discussions

Devices were stored and characterized under nitrogen ambient. All electrical characterizations were performed usingKeithley 2636A. Transfer characteristics $I_D$-$V_{GS}$ were plotted at room temperature. All the measurements were carried out in the same conditions, the gate-source voltage $V_{GS}$was varied from -15V to 60V with a 1V step, at constant drain-source voltage $V_{DS}$ (+10V). In these conditions of polarization the transfer curve in linear regime can be plotted. Output characteristic $I_D$-$V_{DS}$were plotted while $V_{DS}$was varied from 0 to 70 V with 2V step and $V_{GS}$ was varied from 0 to 60V with 10V step.

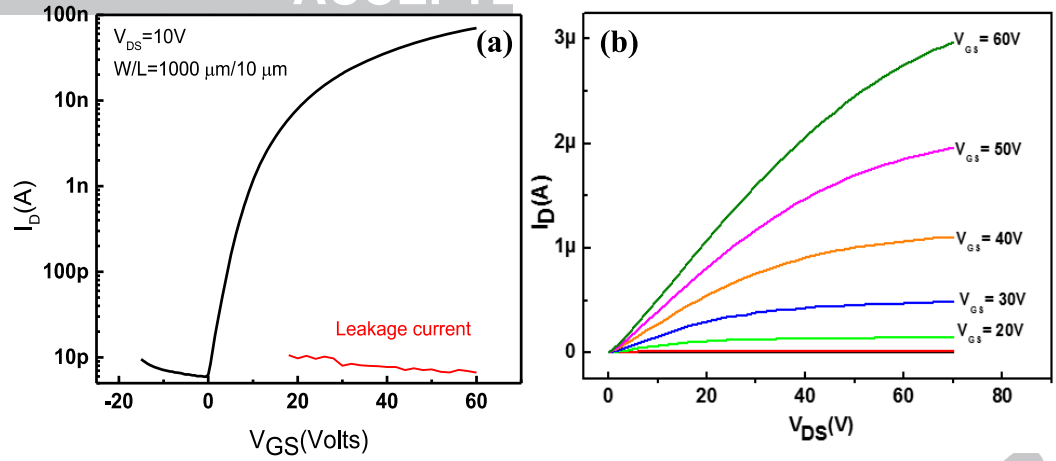


Figure 2: (a) Transfer characteristic at VDS=10V and (b) Output characteristic of IF$(CN_2)_2$meta based OTFT

Transfer and output characteristics of W/L=1000µm/10µm transistors are given in Figure 2. Organic transistors performed at $T_{sub}$=30°C with a fixed deposition rate $d_r$=0.4A°/s show field effect behavior. Negligible OFF current about 10pA is observed at $V_{GS}$= -15 V, confirming a low injection of minority carriers into the active layer owing to theIF$(CN_2)_2$ metamolecule's large band gap. The good insulating property of SU-8 insulator is confirmed with a low leakage current $I_G$ limited at 10pA at $V_{GS}$=60 V.

Linear field effect mobilityis calculated using MOSFET equations in a linear regime ($V_{DS}$<<$V_{GS}$-$V_{TH}$) equation (1).

$$I_D = \frac{W}{L}\mu_{FE}C_{ins}(V_{GS} - V_{th})V_{DS} \quad (1)$$

Where W and L are the width and length of the channel, $\mu_{FE}$ is the field effect mobility, $C_{ins}$ is the gate insulator capacitance per area unit here $C_{ins}$=7.6nF/cm$^2$, $V_{TH}$is the threshold voltage and $V_{DS}$ is applied source drain voltage. Field effect mobility is calculated from transconductance $g_m$ given by:

$$g_m = \left\{\frac{\partial I_{DS}}{\partial V_{GS}}\right\}_{V_{DS}=cte} = \mu_{FE}\frac{WC_{ins}V_{DS}}{L} \quad (2)$$

The calculated field effect mobility was found to be $\mu_{FE}$ = (1.5±0.2) x $10^{-4}$ $cm^2$/V.s, this value is average on devices possessing W/L=1000 µm/10 µm. This transistor length was selected to represent the present device performances, in order to avoid any access resistance effect.

The obtained mobility is quite low compared to reported mobility for indenofluorene derivatives [21, 22]. This low mobility may result from the amorphous feature of evaporated $IF(CN_2)_2$ meta film in the actual deposition parameters.

### 3.1 . Active layer optimization

In an effortto improve the obtained field effect mobility, we investigated a study on the evaporation process. Indeed parameters such as deposition temperature($T_{sub}$) and deposition rate($d_r$) were varied and their impact on the mobility was evaluated. Therefore, we focused on the conditions of the active layer evaporation.We believe that the condition key to obtain high field effect mobility is the control of the films growth process;highly ordered molecular structuresmay lead to a fluent transport of carriers over the π-conjugated system. Moreover, to the best of our knowledge, the effect of evaporation conditions on $IF(CN_2)_2$ meta molecule's morphology has never been studied.

To highlight the first parameter effect; substrate temperature during molecule evaporation, we fabricated 6 groups of devices exactly in the same conditions. During molecule evaporation the deposition rate and films thickness were fixed for all devices at $d_r$=0.4A°/s, and 8nm respectively. Substrate temperature was varied from 30 °C for the 1$^{st}$group to 110 °C for the 6$^{th}$ group.

In Figure 3 we represent the mean field effect mobility corresponding todifferent substrate temperatures. Triangular marks represent mean field effect mobility values average on10

devices possessingsamechannel width and two different lengths ;W=1000µm and L={10,20}for each specific substrate temperature.

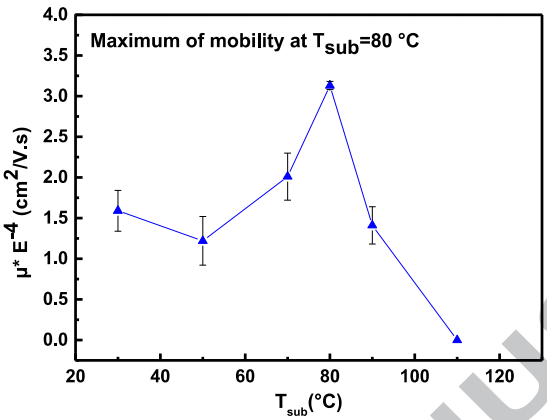


Figure 3: $\mu_{FE}$vs $T_{sub}$representation at $d_r$=0.4A°/s

The data analysis denotes some differences and trends. In fact the field effect mobility remains unchanged from 30°C to 60°C, then increases gradually from 70°C reaching its maximum value at 80°C. From 80°C the mobility tends to decrease, until it strongly deteriorates at 110 °C.

The maximum value of $\mu_{FE}$obtained at $T_{sub}$=80°C is 3.2x$10^{-4}$ $cm^2$/V.sand the averagevalue is $\mu_{FE}$= (3.1±0.05)x$10^{-4}$$cm^2$/V.s.Therefore the final mobility value doubles comparing to obtained value at $T_{sub}$=30 °C.

The present evolution of mobility according to substrate temperature$T_{sub}$ is commonly observed in other type of molecules such as Pentacene and DNTT[16-18], where a maximum mobility is obtained for a specific temperature, here 80°C. One can explain this behavior by the molecule grain size. High deposition temperature may results in large grain film structure [28] and since a direct consequence of the grain size was observed on field effect mobility [18,24], we can conclude the effect of deposition temperature on field effect mobility.

The effect of grain size on field effect mobility has been reported for microcrystalline P3HT films [24], where a mobility improvement took place for larger grain size structures. This is commonly explained by a larger crystallized fraction, while the amorphous part reduces. Sincethe carrier transport inside a crystallized grain is fluent, it is obvious that high mobility results from larger grain structure.

On the other hand the substrate on which the active layer grows (here gold and SU-8 insulator) plays a crucial role as well [29]. For this reason we investigated morphological characterizations, using AFM, on the final device. Indeed our bottom gate bottom contact structure is convenient for such processing, that allows us to avoid the effect of bottom layer. Tapping-mode AFM characterization in argon ambient were performed, on three specific samples ($T_{sub}$=30 °C, 80 °C, 110 °C) these strategic samples were selected in order to understand the mobility behavior according to substrate temperature.

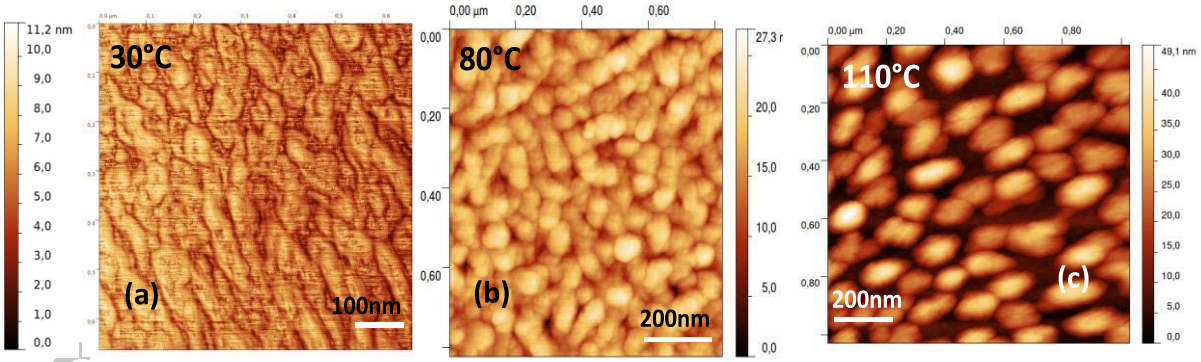


Figure 4: AFM images on films deposited at (a) $T_{sub}$=30°C, (b) $T_{sub}$=80°C, (c) $T_{sub}$=110°C

Images provided by AFM are reported in(Figure.4),the extracted average grain sizes are 50nm, 60nm and 100nm for 30 °C, 80 °C and 110 °C respectively. This result indicates an increase in average IF $(CN_2)_2$ meta grain size when $T_{sub}$ rises from 30 °C to 110 °C, and may explain the mobility improvement at 80 °C. To support this observation, TEM (Transmission Electron Microscopy) measurements were performed on IF $(CN_2)_2$meta filmsdeposited at 30°C and 80°C.

In Figure.5 we report TEM images for both samples, used TEM grids are made of carbon rending the distinction between the carbon grid and the organic active layer difficult. However wecould notice the presence of crystallized zones (red circles Figure.5) on IF $(CN_2)_2$meta films.These crystallites consist of highly ordered molecular planes with preferred orientation, the distance between two successive molecular planes is comprised between 0.74-0.84 nm. The obtained inter-plane distance is consistent with the planarity of present IF $(CN_2)_2$ meta molecule, in fact this short distance involved a good π-π stacking of molecular planes which promotes the carrier transport in the system.

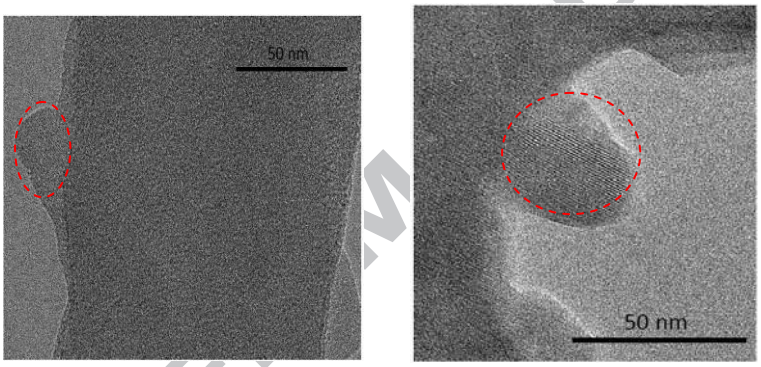


Figure 5 : TEM images on IF$(CN_2)_2$films ; left ($T_{sub}$=30°C) , right ($T_{sub}$=80°C)

Further characterizations were performed on the same samples using electronic diffraction, results are given in Figure 6.Obtained diffraction rings highlight the microcrystalline structure of IF$(CN_2)_2$ metafilms, moreover we notice that diffraction profile for films deposited at 30°C does not allow to distinct clear and separated rings corresponding to molecular planes. Whereas the diffraction profile of films deposited at 80°C consists of slightly clear and distinct rings, indicating a higher crystalline fraction of films deposited at $T_{sub}$=80°C. Thus we can correlate and explain the increase of transistors mobility by an enlargement of crystalline fraction of IF$(CN_2)_2$ meta filmsdeposited at 80°C.

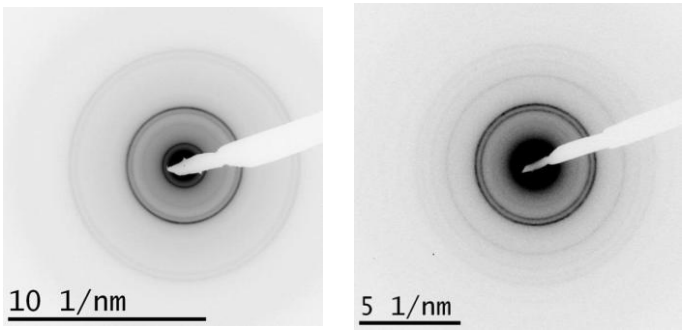


Figure 6: Electronic diffraction rings on $IF(CN_2)_2$ films; left ($T_{sub}$=30°C) ,right ($T_{sub}$=80°C)

On the other hand we remind the transistor's mobility decrease from $T_{sub}$=80 °C Figure 3. The mobility deterioration, is surprising since AFM images revealed a large grain size of 100 nm at $T_{sub}$=110 °C Figure 4. We assume the grain size enlargement at high $T_{sub}$ being due to high diffusion mechanism during films growth [28]. Nevertheless the mobility decrease despite the large grain size at $T_{sub}$=110 °C can be explained by the weak overlapping between the neighboring grains observed in Figure 4(c).Indeed we remember films thickness was fixed at 8nm, therefore enlarging the size of grains leads to reducing the overlapping between them until the film becomes discontinued. In this case (Figure 4 (c)) it seems that charge transport from one grain to the next one is extremely difficult.

In order to confirm this supposition we performed Conducting-AFM measurements on $IF(CN_2)_2$ meta filmswhile evaporated at $T_{sub}$=110°C on gold substrate, AFM measurements are performedunder inert argonambient.Figure 7 (b) represents the morphology of films deposited at 110°C (already shown in Figure 4(c)).Figure 7 (a)gives I-V characteristics while the AFM probe is focused on one isolated grain (green curve) and between two successive grains (red curve). It seems that no electrical conduction exists between successive grains, unlike inside one grain where an electrical current is detected Figure 7 (a) (green curve). This measure confirmsour hypothesis which stipulates that at $T_{sub}$=110°C, $IF(CN_2)_2$meta grains are totally separated and no carrier transport occurs. In their work Y.-Y.Lin et al[25] observed the

same phenomenon on 30nm thick pentacene, at $T_{sub}$=90°C dendritic pentacene grains were formed but separated by voids too restrictive for thecarrier's mobility. To overcome this problem Lin and coworkers suggested a stacked structure, where first 30nm pentacene layer is deposited at 90°C followed by a second pentacene layer deposited at lower temperature, in order to fill voids and recover the film continuity.This way may be a solution in our case to avoid the discontinuity between grains and increase $\mu_{FE}$of carriers at $T_{sub}$=110°C.

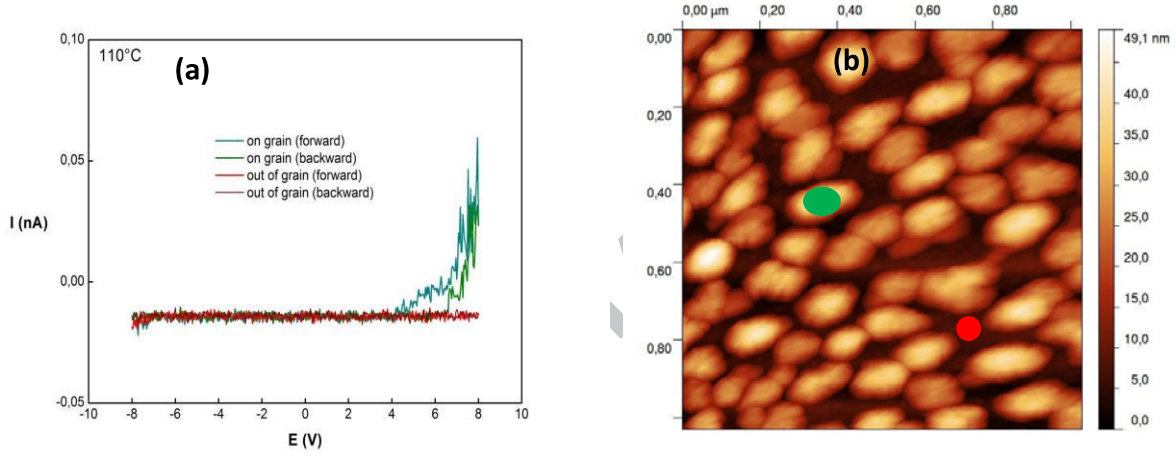


Figure 7 : (a) C-AFM measurements, (b) morphology of $IF(CN_2)_2$meta deposited at 110°C

The second deposition parameterwhich may have an impact on carriers mobility (hence $\mu_{FE}$) is the deposition rate, in the same way as substrate temperature effect,the effect of $d_r$has been reported for a wide range of molecules [18,19].

According to previous results related to $T_{sub}$ effect, $IF(CN_2)_2$meta molecules are thermally evaporated at fixed $T_{sub}$=80°C, with fixed thickness of 8nm. The deposition rate of $IF(CN_2)_2$ meta is varied from 0.1A°/s to 2A°/s. After characterization of corresponding organic TFTs, we evaluated how the deposition rate affects their field effect mobility. Figure 8 shows the evolution of mean $\mu_{FE}$according to the deposition rate. The data analysis reveals some trends, it seems thatfield effect mobility increaseswith increasing $d_r$until reaching a maximum meanvalue $\mu_{FE}=(3.5\pm0.4)x10^{-4}cm^2/V.s$ at $d_r$=0.7A°/s, then declinesfor higher $d_r$.

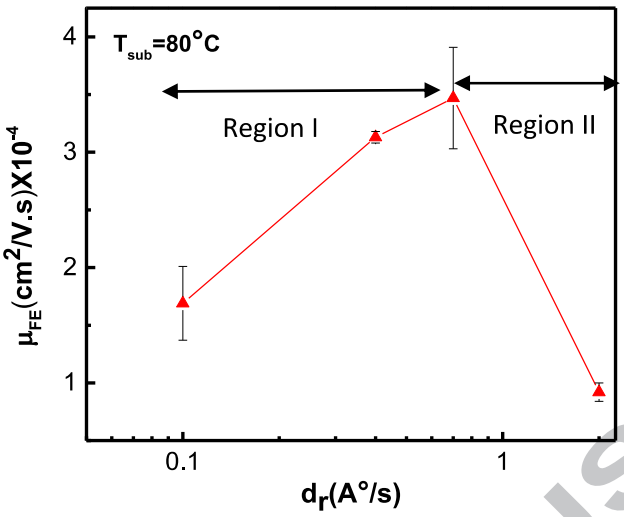


Figure 8: Evolution of the field effect mobility as a function of deposition rate

To explain this behavior, one has to take a closer look to the dynamic growth of $IF(CN_2)_2$meta molecule. It was already reported that the mobility has a proportional relationship with packing density of organic molecules[26,27]. At low deposition rates the packing density N of $IF(CN_2)_2$ meta increases when the deposition rate rises following the scaling relation:

$$N \sim \left(\frac{d_r}{D}\right)^{\chi} \quad (3)$$

Where D is the diffusion coefficient correlated to substrate temperature, and $\chi$ is the scaling exponent defined in [28].

To evaluate the packing density in our films TEMmeasurements are performed on 0.1A°/s and 2A°/s samples, resulted images are reported in Figure 9. At a fixed $T_{sub}$ the diffusion coefficient D is constant, for low $d_r$ (Region I);adatoms diffuse at the surface to form islands,this low molecule flow (hence low deposition rate)permitsthe growth of large grains (>200nm) with low packing density structure as shown in Figure 9 (a). Thus low field effect mobility results for low packing density.

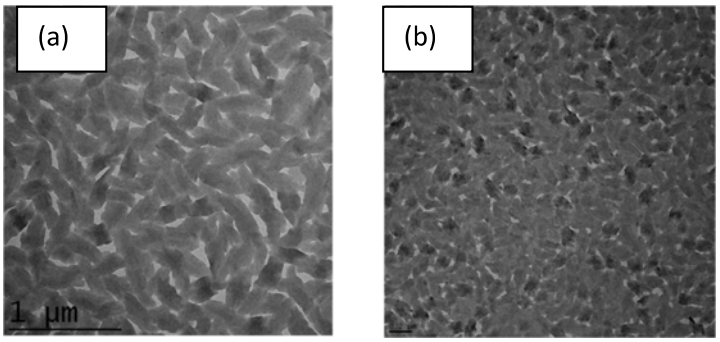


Figure 9: TEM images performed on films deposited at$d_r$=0.1A°/s(a) and $d_r$=2A°/s (b)

With increasing $d_r$, both packing density N and the overlapping between grainsincreased, enhancing the field effect mobility to an optimum value at $d_r$=0.4-0.7A°/s$\mu_{FE}$ = 3.5x $10^{-4}$ $cm^2$/V.s. In Region II above0.7A°/s the molecule flow (hence low deposition rate) becomes important and the packing density saturated.However at high molecule flow large grains don't have the time to grow and IF$(CN_2)_2$meta grain size considerably decreases to 30nm (Figure 9 (b)). As a result of this small grain structure, the field effect mobility falls to $\mu_{FE}$<$10^{-4}$$cm^2$/V.s(Figure 8).

This study allows us to fix the optimal conditions to deposit IF $(CN_2)_2$ meta film in order to obtain slightly higher field effect mobility. As a consequence the fixed conditions in term of deposition temperature and deposition rate are $T_{sub}$=80 °C and $d_r$=(0.4-0.7) A°/s.

A final post treatment is performed on OTFTs, in which the active layer was deposited at $T_{sub}$=80 °C and $d_r$=0.7 A°/s. This treatment consists of a post-annealing from room temperature to 150°C under nitrogen environment. After a slow cooling to room temperature under the same environment, devices are characterized. Figure 10 shows a transfer characteristic of 1000µm/10µm device before and after annealing treatment. After annealing,linear field effect mobility of devices increases and reached $\mu_{FE}$=(1.1±0.3)x$10^{-3}$$cm^2$/V.s (Figure 10), saturated mobility is found to be 2.2x$10^{-3}$$cm^2$/V.s.Reported work on single crystal indenofluorene films, in which IF core molecule was linked to Ar groups, [21] saturated mobility was $\mu_{sat}$=3x$10^{-3}$$cm^2$/V.s. Here IF$(CN_2)_2$ meta films do not present such film

quality, but show comparable field effect mobility. That highlights the interest of the present $IF(CN_2)_2$ meta molecule comparing to other indenofluorene derivatives.

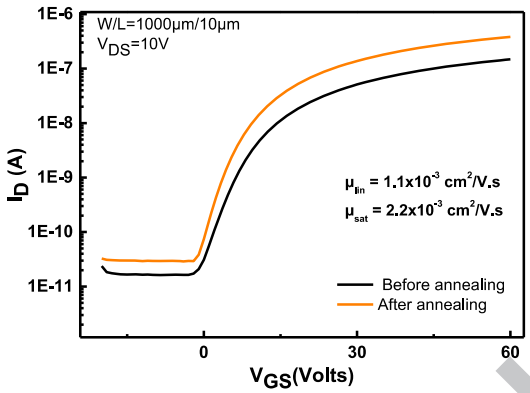


Figure 10 : Transfer characteristic of $IF(CN_2)_2$ organic TFT deposited at $T_{sub}$=80°C and $d_r$=0.7A°/s before and after post-annealing

The field effect mobility improvement after post-annealing treatment can be attributed to one or a combination of the following reasons (1) eliminated vacancies and/or lattice defectsin organic materials, (2)structural rearrangement of IF $(CN_2)_2$meta films (3)better matching at the SU-8/$IF(CN_2)_2$ interface resulting in higher mobility.

### 3.2. Electrical stability of $IF(CN_2)_2$ meta OTFTs

Reached field effect mobility is acceptable for low frequency applications, however for a proper use of the devices, their reliability has to be evaluated. In this section gate bias stress measurements are performed on devices. This test consists on applying a bias voltage on gate electrode to maintain the OTFT in on-regime here called $V_{Gstress}$-$V_{th}$ and about 20V, while drain-source voltage is grounded. At regular intervals of time, the high stress voltage is removed and transfer characteristics are plotted. Here, total duration of stress, is fixed to 3 hours.

As a consequence of the applied gate bias stress, a shifttrend of threshold voltage towards positive values is observed (Figure.11). Two different causes are generally given in order to

explain this $V_{th}$ shift. The first one involves a carrier trapping inside the gate insulator bulk, in this case the $V_{th}$ shift is expected to follow a logarithmic law according to stress time [30].The second cause responsible of the $V_{th}$ shift is explained by defect generation inside the active layer and/or carrier trapping in the active layer/insulator interface, when such phenomenon happens $V_{th}$ shift is described using a strecthed exponential law as a function of stress time [30,31].

Here the obtained $V_{th}$ shift follows a logarithmic law [23] (Figure.11 (a)), which may indicate a carrier trapping phenomenon inside the active layer. The maximum $V_{th}$ shift is about 9 V after 3 hours of 20V applied gate bias stress, this shift is acceptable comparing to reported shifts for OTFTs devices. Moreover we report a very stable field effect mobility and substhreshold slope during the applied stress (Figure.11 (b)) which is coherent with the insulator trapping carrier more than defect generation mechanism [23]. The absence of defect generation mechanism under gate bias stress reflects the stability of the present active layer made of $IF(CN_2)_2$ meta molecule.

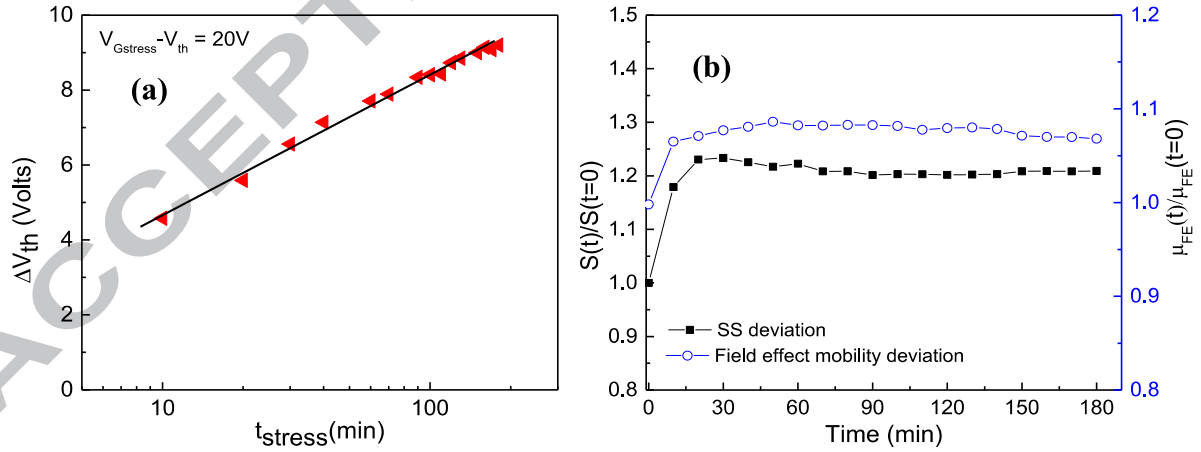


Figure 11 :(a) $V_{th}$ shift and (b) Suthreshold slope and field effect mobility evolutions as a function of stress time

In the next section optimized devices are combined to P channel OTFTs in order to perform CMOS inverter circuit.

### 3.3.CMOS organic inverter

The inverter schematic and its cross section are shown on Figure 12. Tips-Pentacene transistors were fabricated as the P channel part, 20nm of Tips-Pentacene layer were thermally evaporated at $T_{sub}$=30°C, $d_r$=0.4A°/s. Transfer and output curves of performed transistors can be shown in Figure 13. Both P and N channel transistor's characteristics are summarized in Table 1.

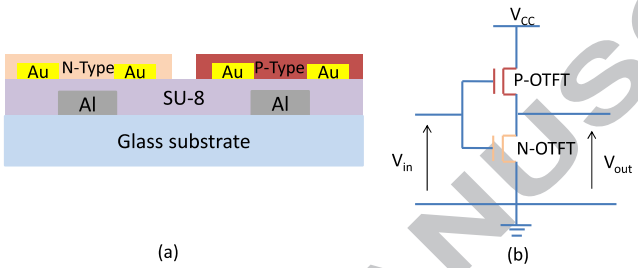


Figure 12 :(a) Cross section and (b) schematic representation of performed inverter

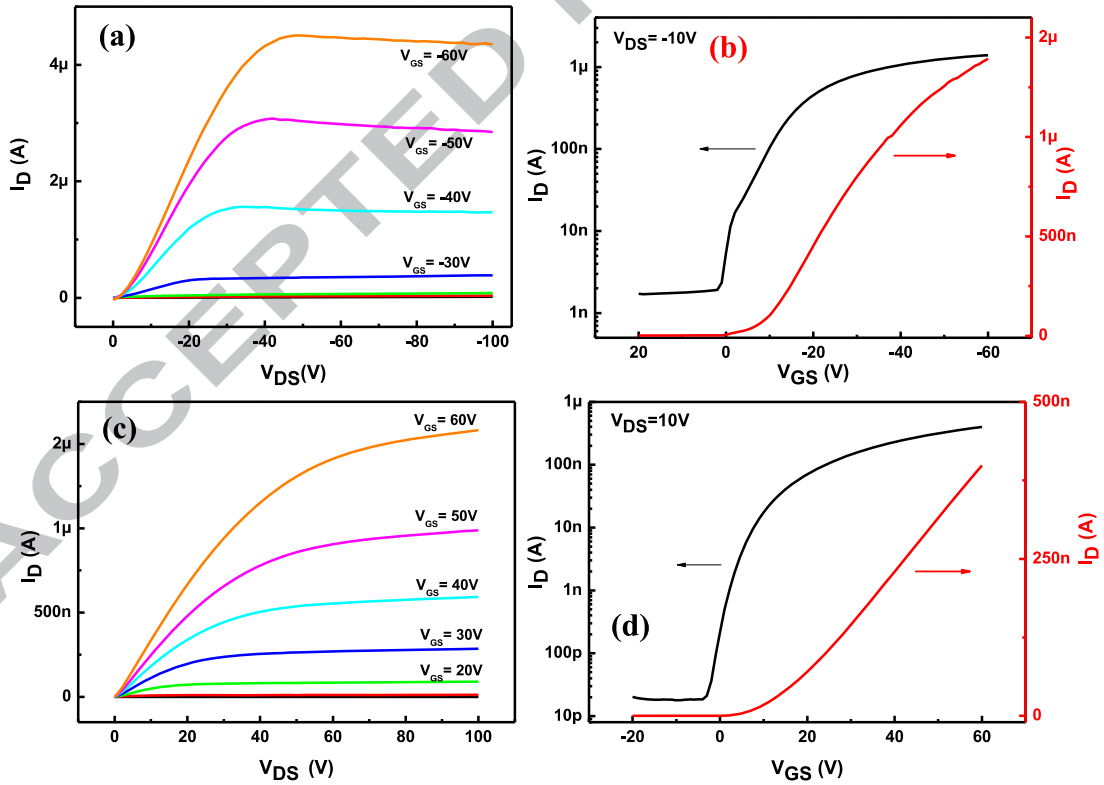


Figure 13 :(a) &(c) : Output, (b) & (d) Transfer characteristic of P and N channel OTFTs respectively

| | Size (µm/ µm ) | $\mu_{sat}(cm^2/V.s)$ | $V_{TH}(V)$ | SS(V/dec) |
|---|---|---|---|---|
| N-channel | 1000/5 | 2.2x10-3 | 7.7 | 2.9 |
| P-channel | 1000/20 | 0.03 | 12.3 | 2.8 |

Table I : Summarized characteristics of performed devices

On the inverter schematic Figure12 (b), the input voltage $V_{IN}$ is biased on the common gate of both P and N channel transistors. Different supply voltages $V_{CC}$ and $V_{IN}$ are applied to the circuit, $V_{OUT}$ corresponding to the inverter response is reported as the Voltage Transfer Characteristic (VTC) in Figure 14(a).

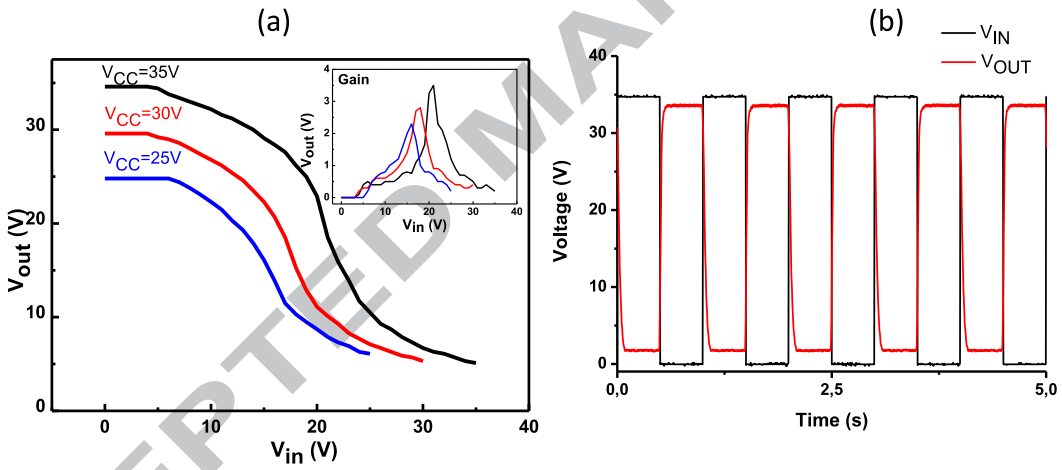


Figure 14: (a) VTC of performed inverter (b) Dynamic characteristic of inverter at f=1Hz

We can observe that at $V_{CC}$=35 V, the output voltage swing OVS ($V_{out}^{MAX} - V_{out}^{MIN}$) = 30 V which represents 85% of applied $V_{CC}$. In Figure.14 (a) we note that for different $V_{CC}$ , while the input voltage $V_{IN}$ is at a minimum value 0V, the output voltage $V_{OUT}$ is maximum $V_{OUT}$=$V_{CC}$. However for a maximum input voltage $V_{IN}$=$V_{CC}$, the output voltage $V_{OUT}$ is about 5V and not connected to the ground 0V. this can be explained by the relatively high OFF current generated by the P type OTFT (about 2nA at 20V Figure.13 (b)). Therefore the

NMOS TFT is not totally pulled to the ground, and the CMOS inverter is not completely switched off.

The decrease rate of $V_{OUT}$ gives the gain (G = $\frac{dV_{OUT}}{dV_{IN}}$) found here to be 3.5. The minimum required gain to perform more complex circuits, such as oscillators is 1, therefore the obtained gain can be considered high enough. Note that the switching threshold voltage here called $V_M$ is obtained at $V_{IN}$=21V when $V_{CC}$=35V, this can be explained by TFT size difference. Knowing that $V_M$ strongly depends on the TFT size, the β factor has to be considered (equation.4)

$$\beta_{n,p} = \mu_{n,p} \frac{W_{n,p}}{L_{n,p}} \quad (4)$$

μ, W and L correspond to transistor's field effect mobility, width and length respectively. The index n/p refers to the TFT type. It is known that when $\beta_n/\beta_p$=1, $V_M$=$V_{CC}$/2 . For the present TFT $\beta_n/\beta_p$=0.2<1, consequently $V_M$ is expected to be larger than $V_{CC}$/2 which explains our $V_M$=21V for $V_{CC}$=35V. The choice of such TFT size was initially motivated by the current modulation regarding the relatively important mobility difference between N and P type OTFTs (Table.1).

A dynamic response of the inverter is also represented on Figure14 (b) at f=1Hz and $V_{CC}$=35V. A sharp switching time is observed for both rising edge and falling edge, in fact when $V_{IN}$ is 35V $V_{OUT}$ is 1.6V, which approaches 0V, and when $V_{IN}$ switches to 0V $V_{OUT}$ switches in a sharp way to 33.7V. The peak to peak magnitude of $V_{OUT}$ is 31.9 V which represents more than 90% of applied $V_{CC}$. Here the operating frequency is f=1Hz, our inverter can be compatible with applications regarding to human body activities, which do not require high operating frequency as temperature sensing or heartbeat detection. However these applications can be considered only if the used circuit is electrically stable enough. To this purpose the electrical stability of our CMOS inverter has been evaluated, in fact when

$V_{CC}$=25V is applied on the circuit during 3 successive hours, the peak to peak magnitude of $V_{OUT}$= 23.1 V decreases to $V_{OUT}$=22.5 V which represents a loss ofonly 2.6 %. This correct stability is a result of good electrical stability of both P and Nchannel used devices.

**CONCLUSION**

In summary we reported an optimization work on $IF(CN_2)_2$ meta based transistors. This study includes the effect of deposition parameters of $IF(CN_2)_2$ meta films on OTFTs field effect mobility. Best evaporation parameters of the active layer were found to be $T_{sub}$=80°C and $d_r$=0.4-0.7A°/s for $IF(CN_2)_2$ meta molecule. This optimum was explained by the best compromise between the IF $(CN_2)_2$ meta grain size and the packing density for using those parameters. Owing to this optimization and the final post annealing treatment the field effect mobility was improved by 20 times from $10^{-4}$ $cm^2$/V.s to $2.2x10^{-3}$ $cm^2$/V.s. Despite the mycrocristalline quality of obtained IF $(CN_2)_2$ meta films, the final field effect mobility is almost equivalent to mobility reported for other indenofluorene derivative with single crystalline quality [21]. Under gate bias stress measurement the devices show a very stable field effect mobility and a correct $V_{th}$ shift. These encouraging results lead us to build CMOS inverter circuit using fabricated IF $(CN_2)_2$ meta TFTs, the circuit exhibits a gain of 3.5 and shows sharp inversion times when operating at 1Hz. Because circuits stability is not provided inmost of articles, here the invertor was continuously polarized at 25V for 3 hours and the peak to peak value decreases only by 2.6%.

**REFERENCES**

[1] A. Reuveny, T. Yokota, T. Sekitani, and T. Someya, “Ultra-flexible short-channel organic field-effect transistors,” *Appl. Phys. Express*, vol. 8, no. 9, p. 091601, 2015.

[2] W. Deng, X. Zhang, J. Wang, Q. Shang, C. Gong, X. Zhang, Q. Zhang, and J. Jie, “Very facile fabrication of aligned organic nanowires based high-performance top-gate

transistors on flexible, transparent substrate," *Org. Electron. physics, Mater. Appl.*, vol. 15, no. 7, pp. 1317–1323, 2014.

[3] V. Raghuwanshi, D. Bharti, and S. P. Tiwari, "Flexible organic field-effect transistors with TIPS-Pentacene crystals exhibiting high electrical stability upon bending," *Org. Electron.*, vol. 31, pp. 177–182, 2016.

[4] J. W. Chung, Y. H. Ko, Y. K. Hong, W. Song, C. Jung, H. Tang, J. Lee, M. H. Lee, B. L. Lee, J. Il Park, Y. Jin, S. Lee, J. S. Yu, J. Park, and S. Kim, "Flexible nano-hybrid inverter based on inkjet-printed organic and 2D multilayer MoS2thin film transistor," *Org. Electron. physics, Mater. Appl.*, vol. 15, no. 11, pp. 3038–3042, 2014.

[5] E. Sowade, K. Y. Mitra, E. Ramon, C. Martinez-Domingo, F. Villani, F. Loffredo, H. L. Gomes, and R. R. Baumann, "Up-scaling of the manufacturing of all-inkjet-printed organic thin-film transistors: Device performance and manufacturing yield of transistor arrays," *Org. Electron. physics, Mater. Appl.*, vol. 30, pp. 237–246, 2016.

[6] G. S. Ryu, K. H. Park, W. T. Park, Y. H. Kim, and Y. Y. Noh, "High-performance diketopyrrolopyrrole-based organic field-effect transistors for flexible gas sensors," *Org. Electron. physics, Mater. Appl.*, vol. 23, pp. 76–81, 2015.

[7] M. Mirza, J. Wang, L. Wang, J. He, and C. Jiang, "Response enhancement mechanism of NO2 gas sensing in ultrathin pentacene field-effect transistors," *Org. Electron.physics, Mater. Appl.*, vol. 24, no. 2, pp. 96–100, 2015.

[8] S. Steudel, K. Myny, S. Schols, P. Vicca, S. Smout, A. Tripathi, B. Van Der Putten, J. L. Van Der Steen, M. Van Neer, F. Schütze, O. R. Hild, E. Van Veenendaal, P. Van Lieshout, M. Van Mil, J. Genoe, G. Gelinck, and P. Heremans, "Design and realization of a flexible

QQVGA AMOLED display with organic TFTs," *Org. Electron. physics, Mater. Appl.*, vol. 13, no. 9, pp. 1729–1735, 2012.

[9] E.-S. Shin, J.-D. Oh, D.-K. Kim, Y.-G. Ha, and J.-H. Choi, "Performance enhancement of pentacene and F 16 CuPc-based low-voltage devices using cross-linked blend gate dielectrics," *J. Phys. D. Appl. Phys.*, vol. 48, no. 4, p. 045105, 2015.

[10] L. K. Mao, J. C. Hwang, and J. C. Tsai, "Operation voltage reduction and gain enhancement in organic CMOS inverters with the TTC/gelatin bilayer dielectric," *Org. Electron. physics, Mater. Appl.*, vol. 16, pp. 221–226, 2015.

[11] K. Fukuda, T. Sekitani, T. Yokota, K. Kuribara, T. C. Huang, T. Sakurai, U. Zschieschang, H. Klauk, M. Ikeda, H. Kuwabara, T. Yamamoto, K. Takimiya, K. T. Cheng, and T. Someya, "Organic pseudo-CMOS circuits for low-voltage large-gain high-speed operation," *IEEE Electron Device Lett.*, vol. 32, no. 10, pp. 1448–1450, 2011.

[12] X. Gao and Z. Zhao, "High mobility organic semiconductors for field-effect transistors," *Sci. China Chem.*, vol. 58, no. 6, pp. 947–968, 2015.

[13] R. P. Ortiz, H. Herrera, C. Seoane, J. L. Segura, A. Facchetti, and T. J. Marks, "Rational design of ambipolar organic semiconductors: is core planarity central to ambipolarity in thiophene-naphthalene semiconductors?," *Chemistry*, vol. 18, no. 2, pp. 532–43, Jan. 2012.

[14] R. Ponce Ortiz, H. Herrera, R. Blanco, H. Huang, A. Facchetti, T. J. Marks, Y. Zheng, and J. L. Segura, "Organic n-channel field-effect transistors based on arylenediimide-thiophene derivatives.," *J. Am. Chem. Soc.*, vol. 132, no. c, pp. 8440–8452, 2010.

[15] M. Mas-Torrent, P. Hadley, S. T. Bromley, X. Ribas, J. Tarrés, M. Mas, E. Molins, J. Veciana, and C. Rovira, "Correlation between crystal structure and mobility in organic field-

effect transistors based on single crystals of tetrathiafulvalene derivatives.," *J. Am. Chem. Soc.*, vol. 126, no. 27, pp. 8546–53, 2004.

[16] D. J. Gundlach, Y. Y. Lin, T. N. Jackson, S. F. Nelson, and D. G. Schlom, "Pentacene organic thin-film transistors - Molecular ordering and mobility," *IEEE Electron Device Lett.*, vol. 18, no. 3, pp. 87–89, 1997.

[17] Y. Hosoi, D. Tsunami, H. Ishii, and Y. Furukawa, "Air-stable n-channel organic field-effect transistors based on N,N′-bis(4-trifluoromethylbenzyl)perylene-3,4,9,10-tetracarboxylic diimide," *Chem. Phys. Lett.*, vol. 436, no. 1–3, pp. 139–143, Feb. 2007.

[18] R. Hofmockel, U. Zschieschang, U. Kraft, R. Rödel, N. H. Hansen, M. Stolte, F. Würthner, K. Takimiya, K. Kern, J. Pflaum, and H. Klauk, "High-mobility organic thin-film transistors based on a small-molecule semiconductor deposited in vacuum and by solution shearing," *Org. Electron. physics, Mater. Appl.*, vol. 14, no. 12, pp. 3213–3221, 2013.

[19] J. H. Bae, S. D. Lee, and C. J. Yu, "Deposition rate dependent mobility of an organic transistor with an anisotropic polymeric insulator," *Solid. State.Electron.*, vol. 79, pp. 98–103, 2013.

[20] C. Rolin, K. Vasseur, S. Schols, M. Jouk, G. Duhoux, R. Müller, J. Genoe, and P. Heremans, "High mobility electron-conducting thin-film transistors by organic vapor phase deposition," *Appl. Phys. Lett.*, vol. 93, no. 3, pp. 30–33, 2008.

[21] D. T. Chase, A. G. Fix, S. J. Kang, B. D. Rose, C. D. Weber, Y. Zhong, L. N. Zakharov, M. C. Lonergan, C. Nuckolls, and M. M. Haley, "6,12-Diarylindeno[1,2- b ]fluorenes: Syntheses, photophysics, and ambipolar OFETs," *J. Am. Chem. Soc.*, vol. 134, no. 25, pp. 10349–10352, 2012.

[22] Y. Park, J. S. Lee, B. J. Kim, B. Kim, J. Lee, D. H. Kim, S. Oh, H. Cho, and J. Park, "High-Performance Stable n -Type Indenofluorenedione Field-Effect Transistors," *Chem. Mater.*, vol. 23, pp. 4038–4044, 2011.

[23] M. Romain, M. Chevrier, S. Bebiche, T. Mohammed-Brahim, J. Rault-Berthelot, E. Jacques, and C. Poriel, "The structure–property relationship study of electron-deficient dihydroindeno[2,1-b]fluorene derivatives for n-type organic field effect transistors," *J. Mater. Chem. C*, vol. 3, no. 22, pp. 5742–5753, 2015.

[24] G. Horowitz and M. E. Hajlaoui, "Grain size dependent mobility in polycrystalline organic field-effect transistors," *Synth.Met.*, vol. 122, no. 1, pp. 185–189, 2001.

[25] Y. Y. Lin, D. J. Gundlach, S. F. Nelson, and T. N. Jackson, "Stacked pentacene layer organic thin-film transistors with improved characteristics," *IEEE Electron Device Lett.*, vol. 18, no. 12, pp. 606–608, 1997.

[26] J. H. Bae, S. D. Lee, and C. J. Yu, "Deposition rate dependent mobility of an organic transistor with an anisotropic polymeric insulator," *Solid. State.Electron.*, vol. 79, pp. 98–103, 2013.

[27] M. Beigmohamadi, P. Niyamakom, a. Farahzadi, S. Kremers, T. Michely, and M. Wuttig, "Evolution of dislocations in perylene films with thickness and deposition rate," *Phys. Status Solidi - Rapid Res. Lett.*, vol. 2, no. 1, pp. 1–3, 2008.

[28] T.Michely, J.Krug, Islands, Mounds and Atoms, *Springer*, New York 2004

[29] F. a. Yildirim, R. R. Schliewe, W. Bauhofer, R. M. Meixner, H. Goebel, and W. Krautschneider, "Gate insulators and interface effects in organic thin-film transistors," *Org. Electron.*, vol. 9, no. 1, pp. 70–76, 2008.

[30] A. A.Fomani and A. Nathan, "Metastability mechanisms in thin film transistors quantitatively resolved using poststress," *Journal of Applied physics,* vol. 109, no. 084521, pp. 0-6, 2011.

[31] E. Jacques, M. Romain, A.Yassin, S.Bebiche, M. Harnois, T.Mohammed-Brahim, J. Rault-Berthelot, and C. Poriel, "Electron deficient dicyanovinylene-ladder-type pentaphenylene derivative for n-type Organic Field Effect Transistors" *J. Mater. Chem. C*, vol. 2, no.17, pp. 3292–3302, 2014.

Highlights:

Organic thin film transistor, indenofluorene molecule, Organic CMOS inverter.

Keywords: Organic electronics,
indenofluorene,
Electrical stability,
CMOS inverter